JOURNAL OF GEOPHYSICAL RESEARCH, VOL. 114, A06318, doi:10.1029/2008JA013931, 2009

Brightening of 630.0 nm equatorial spread-F airglow depletions

Carlos Martinis,[1] Jeffrey Baumgardner,[1] Michael Mendillo,[1] Shin-Yi Su,[2] and Nestor Aponte[3]

Received 21 November 2008; revised 6 February 2009; accepted 14 April 2009; published 27 June 2009.

[1] Observations from the Boston University all-sky imaging system at Arecibo, Puerto Rico (18.3°N, 66.7°W, 28°N mag), show an unusual behavior of nighttime 630.0-nm airglow depletions. Associated with equatorial spread-F (ESF), these structures move eastward before reversing their motion and become airglow enhancements. Few other cases have been found, all during December solstices. For the case study presented here, data from the Arecibo incoherent scatter radar and the Republic of China Scientific Satellite (ROCSAT-1) provide supporting information. The radar shows that around local midnight the background zonal and meridional plasma motions reverse to westward and southward, respectively. ROCSAT-1 shows enhanced ion density, i.e., a low-latitude plasma blob, above the bright feature recorded by the all-sky imager, indicating a possible connection between both phenomena. Drifts parallel to the magnetic field are observed only in the region where the enhancement occurs. One possible interpretation of this change in the brightness of the depleted structure involves the influence of northward meridional winds and a reversal in the zonal drift motion, most likely caused by a zonal wind reversal.

Citation: Martinis, C., J. Baumgardner, M. Mendillo, S.-Y. Su, and N. Aponte (2009), Brightening of 630.0 nm equatorial spread-F airglow depletions, *J. Geophys. Res.*, *114*, A06318, doi:10.1029/2008JA013931.

1. Introduction

[2] All-sky imaging techniques have been shown to be extremely valuable when studying the evolution of processes in the mesosphere, thermosphere, and ionosphere. Images help to better understand processes occurring in the upper atmosphere by literally adding a second observational dimension to line-of-sight (e.g., radar) or in situ (e.g., rocket and satellite) measurements. When conducted in concert with such diagnostics, comprehensive multiparameter studies emerge.

[3] The Boston University all-sky imager at Arecibo, Puerto Rico, was installed in 2002. This site is poleward from the northern crest of the Equatorial Ionization Anomaly (EIA) and therefore is susceptible to processes driven by low-latitude and midlatitude electrodynamics. The inclination of the terrestrial geomagnetic field ($I \sim 45°$) also makes it optimal for ionospheric effects driven by thermospheric winds that seem to play a crucial role in the phenomena described here. Among the many perturbation effects involving electric fields and winds are medium-scale traveling ionospheric disturbances (MSTIDs) [*Hunsucker*, 1982; *Garcia et al.*, 2000; *Shiokawa et al.*, 2003] and airglow brightness waves (BW) associated with the midnight temperature maximum (MTM) [*Mendillo et al.*, 1997]. At Arecibo, MSTIDs are seen by all-sky imagers as well defined dark or alternating dark/bright bands moving southwestward at a large angle with respect to the geomagnetic meridian [*Mendillo et al.*, 1997; *Miller et al.*, 1997; *Garcia et al.*, 2000]. These features were initially related to the Perkins instability [*Perkins*, 1973; *Behnke*, 1979; *Kelley et al.*, 2002] but, recently, a more likely mechanism involving the coupling between sporadic E (Es) layer and *F* region instabilities is thought to play a significant role [*Cosgrove and Tsunoda*, 2004; *Cosgrove*, 2007].

[4] Another process observed at Arecibo, far less frequently but equally dramatic, is the airglow signature of equatorial spread-F (ESF), process associated with a perturbation analog to the hydrodynamic Rayleigh-Taylor instability (RTI). In these cases, depleted regions in 630.0-nm airglow emissions grow in latitude and occasionally reach (and pass) Arecibo's zenith [*Martinis and Mendillo*, 2007, and references therein]. These airglow depletions tend to move eastward. The observation of depletions reaching the zenith at Arecibo implies plasma bubbles moving to altitudes higher than 2000 km at the magnetic equator.

[5] The interpretation of optical airglow features is sometimes complicated by the fact that there is no unique way of obtaining depleted/enhanced airglow signatures. The 630.0-nm airglow emissions arise from the dissociative recombination of O_2^+, itself preceded by the reaction between O^+ and O_2. Its peak emission occurs approximately one scale height below the peak of the *F* layer, between 250 and 300 km, depending, among other factors, on solar activity. Thus

[1] Center for Space Physics, Boston University, Boston, Massachusetts, USA.
[2] Institute of Space Science and Center for Space and Remote Sensing Research, National Central University, Chung-Li, Taiwan.
[3] National Astronomy and Ionosphere Center, Arecibo Observatory, Arecibo, Puerto Rico, USA.

0148-0227/09/2008JA013931$09.00

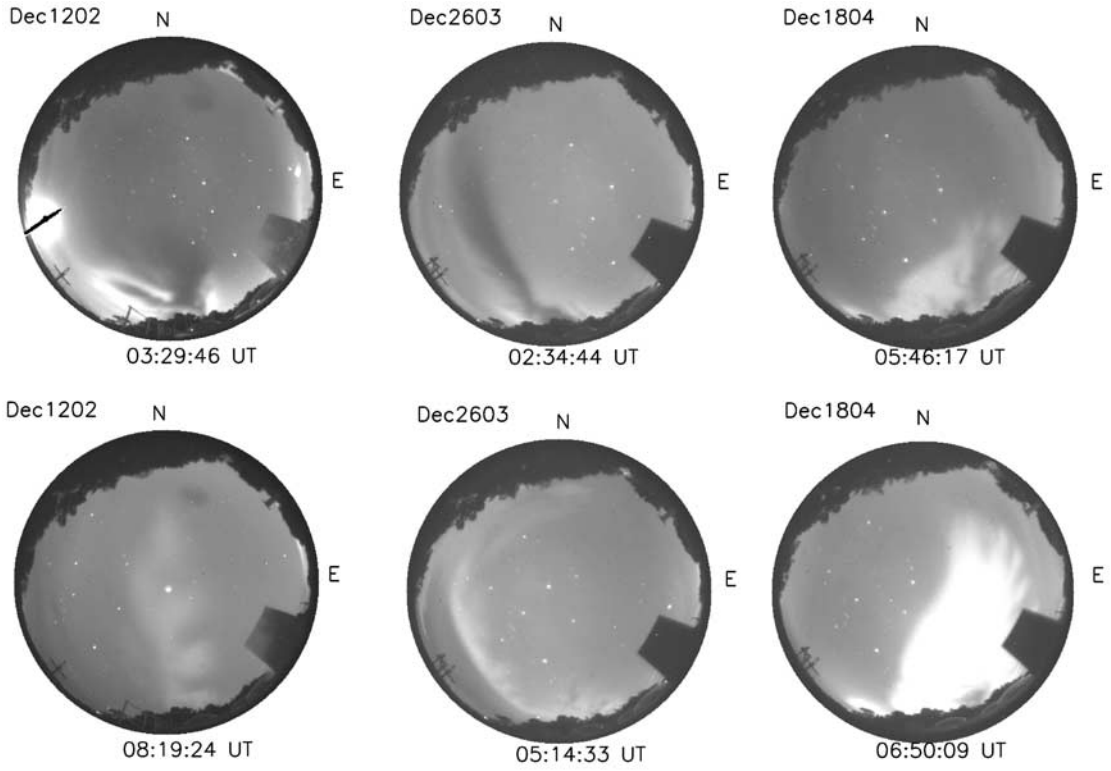

Figure 1. Examples of all-sky images at 630.0 nm for three different nights (12 December 2002, 26 December 2003, and 18 December 2004); (top) initial dark depletions and (bottom) their final stage as bright structures. North is at the top and east is to the right of each image. Obstructions by trees occur on the north and south horizon, with a light-blocking mask in the southeast.

reductions (increases) in airglow emission can be understood as being produced by a decrease (enhancement) in electron density at the height of emission or an upward (downward) motion of the ionospheric layer to regions of lower (higher) O_2 concentration. For the ESF-related structures, airglow depletions are due to reduced electron density at the height of the emission layer. For the bright/dark bands, associated with MSTIDs, the interpretation implies downward/upward motion of the ionospheric layer.

[6] In this study we focus on processes in which ESF-related airglow depletions evolve into enhanced airglow structures after changing the direction of motion from eastward to westward.

2. Data

[7] The Boston University all-sky imager [*Baumgardner et al.*, 1993] at the Arecibo Observatory has been taking data continuously since May 2002. It utilizes a charge-coupled device (CCD), thermoelectrically cooled to $-50°C$. A rotating filter-wheel houses up to six narrowband (1.2–1.8 nm FWHM) filters to record nighttime mesospheric and thermospheric emissions, plus the background continuum. (Quick-look movies and individual frames are available online at www.buimaging.com.)

[8] Figure 1 shows three different nights when dark structures in 630.0 nm (top) moving eastward are seen to develop into bright features (bottom) later in the night. Magnetic the activity was relatively quiet for the three nights, with the SYM-H index less than -15 nT. We interpret the dark structures at the top of Figure 1 as typical ESF airglow depleted regions, the optical signatures of the footprints of depleted flux tubes, a consequence of the equatorial Rayleigh-Taylor instability. The apex height (i.e., the altitude at the magnetic equator of the field line intersecting the airglow layer) of a depleted flux tube in the southern part of the imager's field of view (FOV) is $\sim$1800 km (e.g., in the first and third frames). Figure 1 (middle) shows a dark structure reaching the northern edge of the imager's FOV, implying apex heights of $\sim$2400 km. These features remained in the FOV for many hours, the first two being premidnight events, and the last occurring after midnight. For each case, later in the night, their eastward zonal motion reverses to westward and it is during this reversal when they evolve into the bright structures shown at the bottom. Note also that finger-like features develop in the eastern side, an indication of secondary instabilities. For the 12 December 2002 case (Figure 1, left) a bifurcated depletion is seen embedded in a bright airglow (Figure 1, top). After $\sim$4 hours the entire depletion has evolved into the bright structure seen at the bottom that is now moving westward and shows finger-like structures in its eastern wall. For the 18 December 2004 case (Figure 1, right), there is also bright airglow surrounding the dark structure (shown at 0546 UT). By 0618 UT, the dark structure reaches the same brightness of the surrounding bright region (not shown), and the final structure seen at

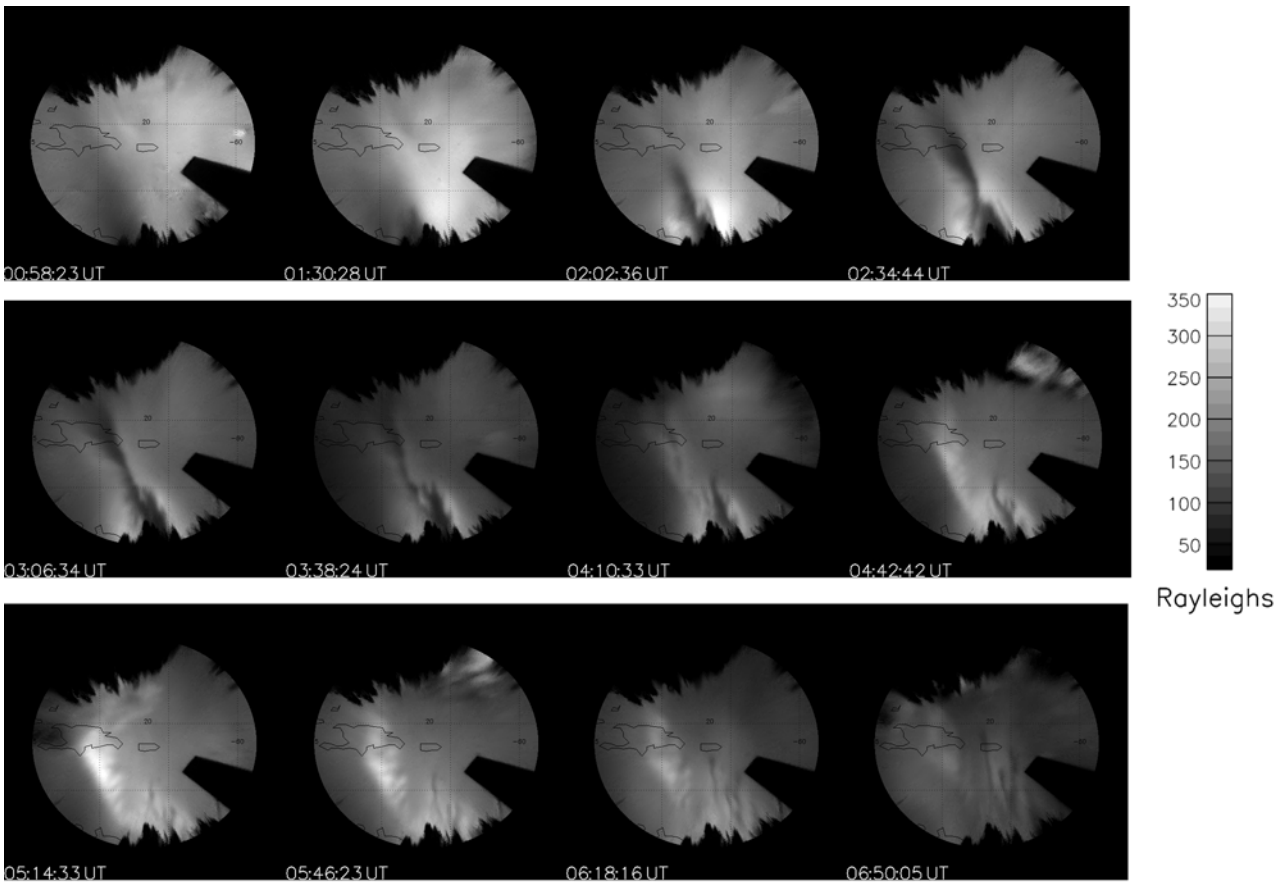

Figure 2. Time evolution of airglow structures on 26 December 2003 from 0058 to 0650 UT. The images have been unwarped, assuming an emission height of 250 km, and are shown in a 150° field of view.

0650 UT consists in a large bright region expanding westward and northward (Figure 1, right, bottom).

[9] In this paper, we analyze the 26 December 2003 (Figure 1, middle) in detail because it shows most clearly the evolution of the dark structure into an enhanced region, and supporting diagnostics from the Arecibo Incoherent Scatter Radar and the Republic of China Scientific Satellite (ROCSAT-1) are available. For this night, SYM-H is less than −5 nT until ∼06:00 UT when it reaches −15 nT. Figure 2 shows a time sequence of 630.0-nm airglow images spanning 0058 UT to 0650 UT, i.e., the premidnight to postmidnight hours. The images have been calibrated into brightness units in Rayleighs (R) using standard stars as reference, and we estimate levels of uncertainty to be ∼25%. Vignetting (the off-axis response of the imaging system that reduces brightness at the rim of the fisheye lens) and Van Rijhn effects (slant path effects that enhance brightness at the rim) were removed. The raw images have been unwarped (i.e., each pixel in the fish-eye image is assigned a geographic latitude and longitude) assuming an emission height of 250 km, with the result shown upon a Mercator map projection. Latitude and longitude grids are at 5° intervals.

[10] Embedded in a bright background, shown in Figure 2 (top), a depletion surges from the south in the western part of the FOV (now reduced to 150°) at 0130 UT and by 0202 UT has reached the latitude of Arecibo's zenith. While slowly moving eastward it reaches a maximum extension at ∼22° geographic latitude at ∼0306 UT. Notice the development of ridges at the western wall, a well known consequence of the wind-driven gradient drift instability [*Tsunoda*, 1983; *Kelley*, 1989]. The elongated dark feature (fully developed by 0234 UT) increases its brightness and by 0442 UT, instead of the typical depletion, a bright structure is clearly observed. It took approximately 2 hours for the reversal to occur. Now the western wall of the bright feature does not show any additional structuring; instead, the eastern wall is the one showing multiple secondary structures. During the entire process, airglow depletions to the south are seen moving eastward. The unusual feature we focus upon is the reversal in brightness of the large depletion that is followed by the development of ridges in its eastern wall.

[11] The Arecibo Radar measured plasma parameters during this night until 0400 UT. Figure 3 shows the maximum electron density, N_{max} (Figure 3, top), and the height of the peak electron density profile, H_{max} (Figure 3, bottom). The apparent temporal periodicity is caused by the azimuth rotation of the Arecibo beam. Nothing unusual is observed during this period above Arecibo, in agreement with the airglow observations at zenith. Ion vector velocities are obtained from line of sight velocity measurements by continuously rotating the antenna beam back and forth 360 degrees in azimuth at 15 degrees off zenith (∼65 km

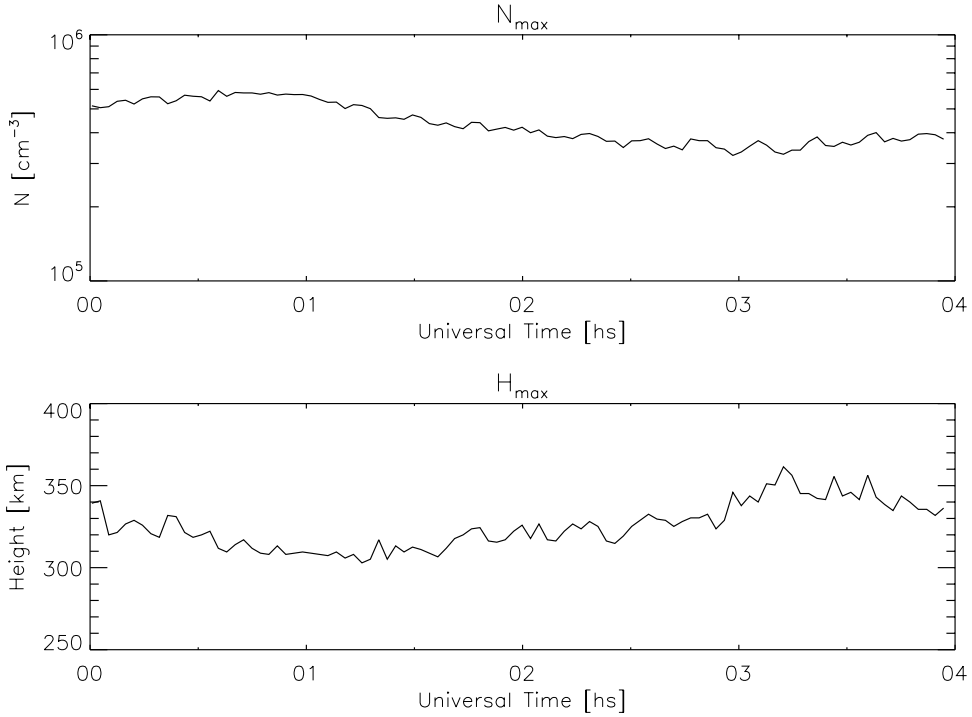

Figure 3. Arecibo Radar measurements on 26 December 2003 between 0000 and 0400 UT. (top) Peak electron density (N_{max}). (bottom) Height of peak electron density (H_{max}). The quasiperiodicity observed is due to the swinging of the beam.

radius at 256 km height) to sample the horizontal components. The processing uses the linear regularization inversion method that instead of assuming the 3D velocities do not change in one rotation (~15 minutes), assumes that the variation between points is linear [*Sulzer et al.*, 2005]. The vector velocities can be obtained in geographical coordinates as V_{south}, V_{east} and V_{up} or in geomagnetic coordinates as V_{paral}, V_{pn} and V_{pe}, the components parallel and perpendicular to the magnetic field in the meridional and zonal planes, respectively. The electric field can be related to the drifts through the relations $E_{pe} = -V_{pn} * B$ and $E_{pn} = V_{pe} * B$. A problem with the Arecibo 430 MHz transmitter (which affects velocities with a vertical component like V_{up} and V_{paral} and V_{pn}) appears to have taken place for these measurements, so we show in Figure 4 horizontal plasma drifts (V_{south} and V_{east}) from 0000 to 0400 UT at two heights: 256 km, representing the height of 630.0 nm airglow emission, and at 516 km, a height closer to the ROCSAT-1 orbit (discussed below). Clearly, at 256 km the background ionospheric plasma over Arecibo reverses its zonal and meridional motions between 0300 and 0330 UT, going from eastward and poleward to westward and equatorward. The reversal for the zonal component seems to occur later at lower altitudes, an indication of the presence of a shear in altitude. The sequence of images in Figure 2 shows that originally the main dark structure observed to the west moves slowly eastward and between ~0330 and 0410 UT it reverses its zonal motion, confirming that it is embedded within and responds to the background conditions measured by the radar. The dark structures to the south of Arecibo's FOV continue their eastward motion until ~06:00 UT. This is a clear indication of the presence of latitudinal shears in the zonal motion of the plasma drifts within the height regime of the 630.0-nm airglow layer.

[12] Two ROCSAT-1 satellite passes (at a height of ~570 km) in the American sector are available for this night. Data were obtained with the Ionospheric Plasma and Electrodynamics Instrument (IPEI), consisting of sensors that measure ion number density, drift velocity vector, temperature, and composition [*Su et al.*, 2001]. The first pass was over South America and the information obtained can be related to the airglow structure observed by the all-sky imager at Arecibo at ~0202 UT. Figure 5a shows a map with the satellite's trajectory and ion density values along it (between 0154 and 0204 UT). The corresponding image from Arecibo shows the elongated dark structure not fully developed. Magnetic longitude lines are indicated to relate both data sets. Because of the flux tube nature of the ESF process the information provided by the satellite can be related to the all-sky imager data assuming that both are sampling the same flux tube at different altitudes/latitudes. A plasma bubble (a factor of ~2 less than the background) is clearly observed by the satellite at a magnetic longitude that is connected to the location of the airglow depletion (~50% darker than the zenith measurements).

[13] Figure 5b shows the next satellite pass in the American sector (between 0353 and 0359 UT), when the structure is becoming brighter than the background (~30% brighter). The pass is directly above the bright feature observed by the imager. The satellite now measures a region of increased ion density (~3 times larger than the background). From Figures 5a and 5b, our interpretation is that the original dark structure, sampled closer to the equator by the satellite as a plasma bubble, has reversed its characteristics to become a bright structure, sampled now by the satellite as

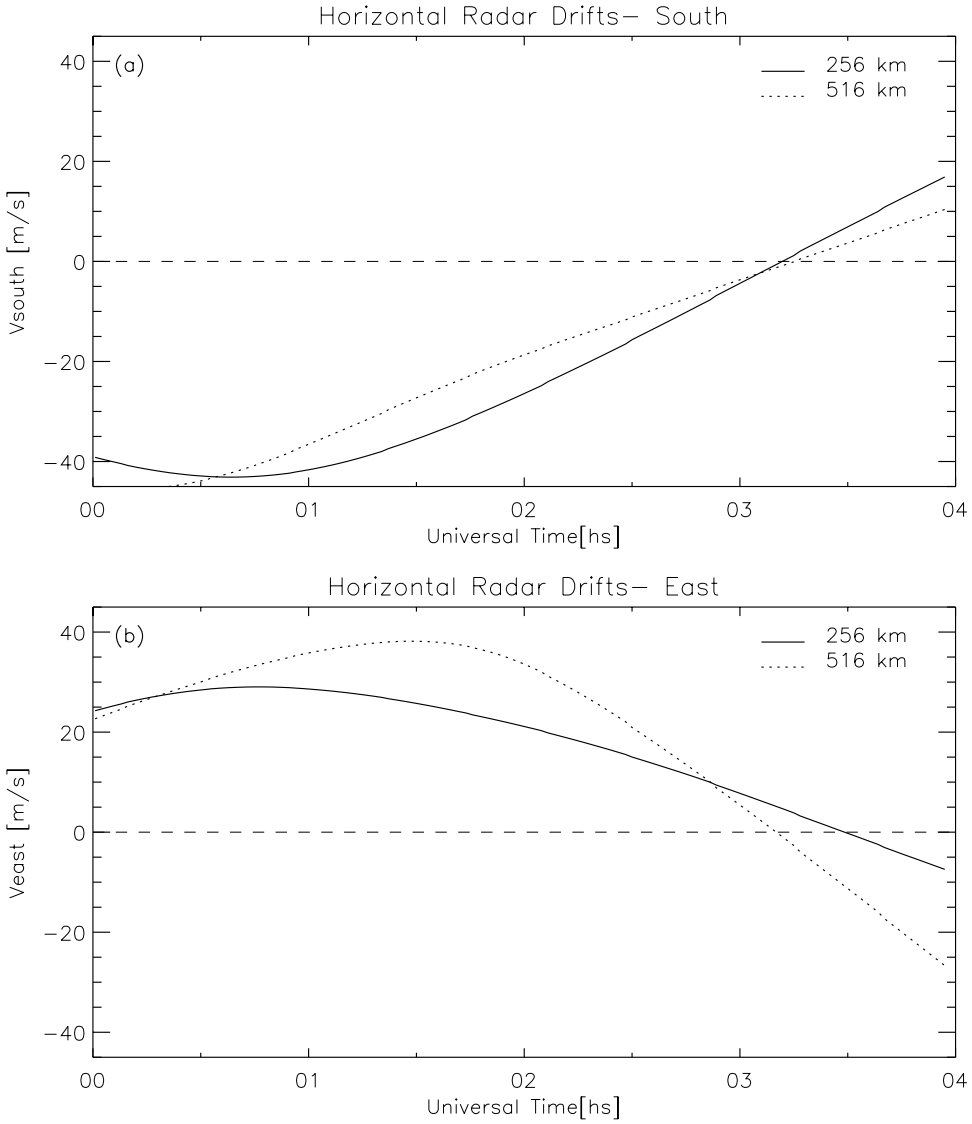

Figure 4. Plasma drifts obtained with Arecibo ISR at 256 km (solid lines) and 516 km (dotted lines). (a) Horizontal drifts in the south (meridional) direction. (b) Horizontal drifts in the east (zonal) direction.

an enhanced ion density region, known as "low latitude plasma blobs" [*Park et al.*, 2003, 2008; *Le et al.*, 2003].

[14] Figure 6 shows ROCSAT-1 plasma velocity components for the second pass in Figure 5b. From top to bottom, Figure 6 shows ion density data; the field-aligned component $V_{||}$ (positive when parallel to the magnetic field, i.e., downward), the perpendicular component in the meridional plane V_{perM} (positive pointing outward, in this case northward), and the perpendicular component in the zonal plane V_{perZ} (positive when pointing eastward). The plasma within the region of density enhancement is slowly moving westward with almost zero meridional motion. Most noticeable is the parallel motion of the plasma: outside the region of the density enhancement the drift is ~ -50 m/s but inside it is $\sim +30$ m/s. This could be an indication of the influence of meridional winds acting in a limited longitudinal sector and producing the enhanced airglow. These results from ROCSAT-1 can be compared with the radar observations of horizontal flow at 516 km in Figure 4, keeping in mind that ROCSAT-1 is measuring perpendicular to B components of the plasma velocity. A very small zonal component is observed (westward flow) while the results for the meridional component show a stronger southward flow as determined by the satellite.

3. Discussion

3.1. Bright Airglow Structures

[15] There is only a brief literature on the contrasting brightness features associated with ESF effects. The airglow signatures that would result from simulations of the Rayleigh-Taylor-like instability at the geomagnetic equator were first computed and compared with observations in the work of *Mendillo et al.* [1985]. The upwelling and downwelling components of ESF flux tubes resulted in depletions versus enhancements to airglow at 630.0 nm versus only depletions for images at 777.4 nm. These enhancements are different from the case shown in the work of *Garcia et al.* [2000]

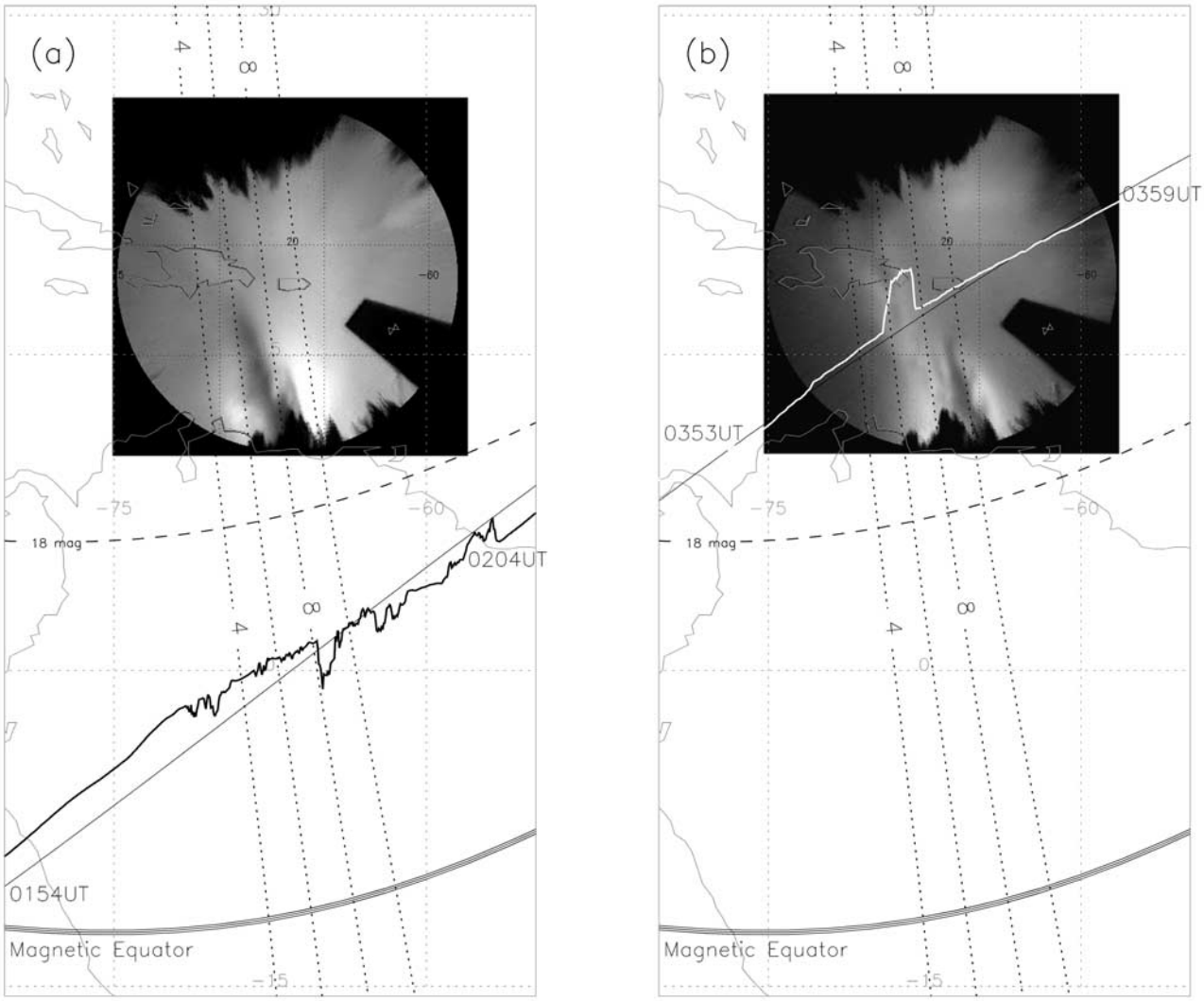

Figure 5. (a) Map showing ROCSAT-1 trajectory and superposed ion density between 0154 UT and 0204 UT. A strong ion density bubble is observed at ~0201 UT close to the geographic equator. Also shown is a 630.0 nm all-sky image (at 0202 UT) with an airglow depletion seen at the same magnetic meridian. (b) Same as in Figure 5a but for the next satellite pass, between 0353 and 0359 UT. The bubble has changed into an ion enhancement, and the all-sky image (at 0410 UT) shows a corresponding airglow enhancement.

where the 630.0 nm emissions during a geomagnetic storm became bright due to the presence of an expanded northern crest of the EIA. Another storm-time study by *Makela et al.* [2006] described a case where ESF airglow depletions are seen surrounded by a bright background airglow, pointing out that the depletions in 630.0 nm keep their characteristics and it is the background airglow layer that is affected by an ongoing geomagnetic storm. Studies by *Pimenta et al.* [2004, 2007] show airglow enhancements occurring simultaneously with airglow depletions, an effect they treat as the bright airglow signatures of plasma blobs. Specifically they consider the mechanism proposed by *Le et al.* [2003] who suggested that the blobs are a consequence of plasma being moved up from the region of the crests of the EIA due to a polarization electric field, associated with the presence of depleted flux tubes. These depletions cannot move to higher latitudes due to field-aligned plasma pressure gradient at their poleward edges. This mechanism assumes that plasma bubbles are limited to occur in the region bounded by the crests of the anomaly; it does not give an explanation for situations in which plasma bubbles reach very high apex altitudes and consequently can be observed poleward of the crests of the EIA. It also implies that blobs should occur near the poleward tip of depleted regions.

[16] Using data from the 47 MHz Equatorial Atmosphere Radar (EAR), *Yokoyama et al.* [2007] observed backscatter plumes associated with plasma bubbles reaching ~13° dip latitude south. The plumes grew upward late in the premidnight sector, in association with the appearance of plasma blobs detected by ROCSAT-1 at dip latitude of ~9° north. Thus the depleted flux tube was limited to regions equatorward of ~9°N and extended to a dip latitude of ~13°S. The authors invoke, following *Le et al.* [2003], the presence of a localized eastward polarization electric field that generates

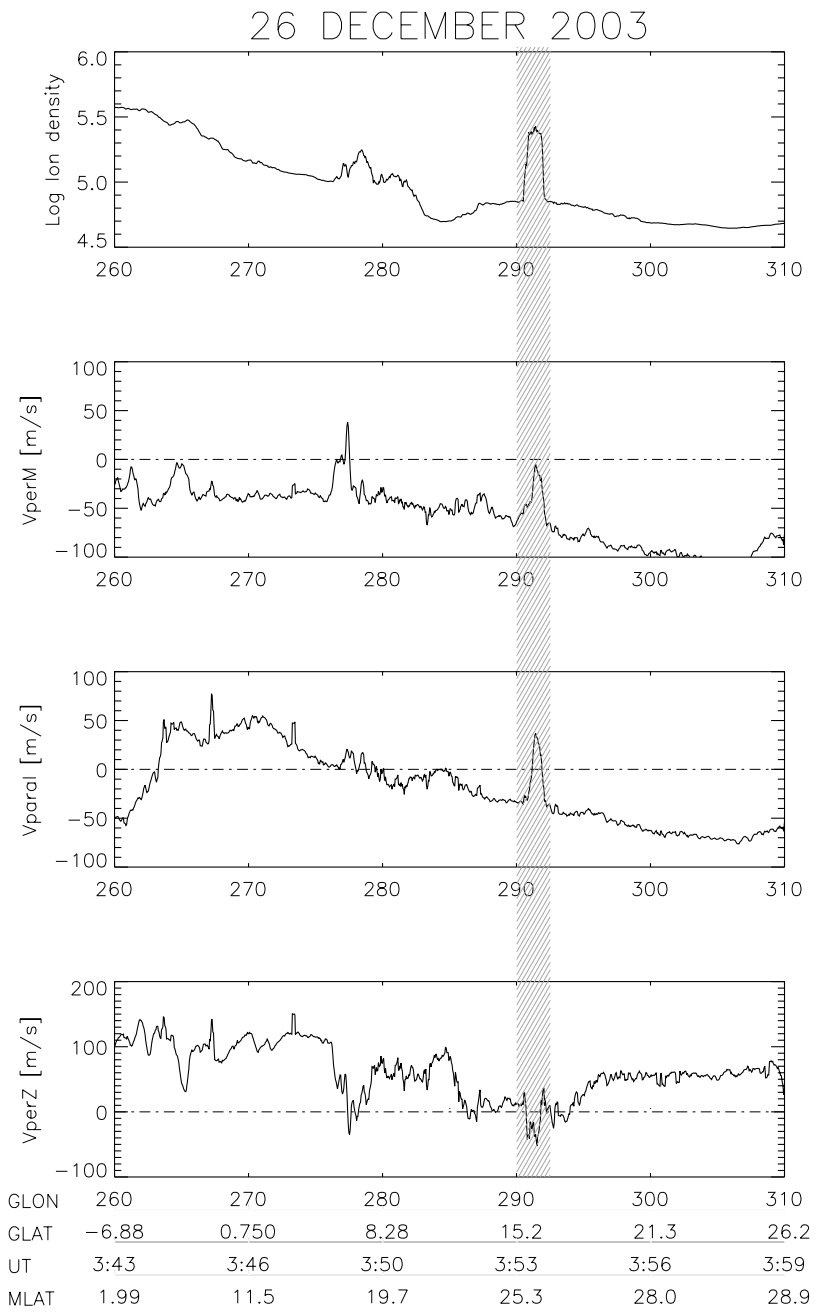

Figure 6. ROCSAT-1/IPEI data for the second pass shown in Figure 5b. The shading indicates the location of the bright airglow structure with associated perturbations in the parameters measured by the satellite. From top to bottom, ion density; perpendicular component in the meridional direction (V_{perM}); parallel component (V_{paral}), and perpendicular component in the zonal direction (V_{perZ}). The salient feature is the presence of strong parallel drifts only in the region of airglow/density enhancement.

plasma blobs as well as the resurgence of the plumes. *Yokoyama et al.* [2007] also point out that the influence of neutral winds might explain the asymmetric development of the depleted flux tube.

3.2. Brightening of Dark ESF Structures

[17] Each of the cases described above did not involve an original depletion evolving into an enhanced feature while the overall background does not change significantly, as reported here. The full set of cases allows us to identify the following additional characteristic features for this phenomenon: (a) an original dark structure, considered to be ESF-related, moving eastward, (b) enhanced background airglow toward the south of Arecibo's FOV, (c) a reversal to westward motion and brightening of the dark structure, (d) occurrence during December solstice period.

[18] The review article on imaging of low-latitude irregularity processes presented by *Makela* [2006] makes reference to the occurrence of these cases where airglow depletions become bright structures, and *Seker et al.*

[2007] showed examples from the nights of 26 December 2003 and 18 December 2004, with no discussion or analysis offered. As shown in Figures 1–6, we are now able to demonstrate that a depleted airglow structure associated with ESF changing into a feature with enhanced airglow is a new and recurrent phenomenon in equatorial and low-latitude aeronomy. Supporting diagnostics allow us to point for the first time to the effect being associated with a reversal in the zonal motion of the background ionosphere and the presence of strong parallel (downward and poleward) drifts that could be associated with of northward meridional winds. Unfortunately, Fabry-Perot interferometer measurements from Arecibo were not available for this night. *Emmert et al.* [2006] showed that average meridional winds at Arecibo during northern hemisphere winter are southward between 2200 and 0000 LT. This pattern is in agreement with the direction of the parallel drifts observed by ROCSAT-1 (antiparallel to B) outside the airglow enhancement region. Inside the structure, parallel to B drifts are observed, that we attribute to a northward neutral wind.

[19] Using the SAMI3/ESF model [*Huba et al.*, 2008], *Krall et al.* [2009] simulated the evolution of the dark structure observed on 26 December 2003. They were able to reproduce the observations by implementing a combination of converging zonal winds and a meridional wind. A steady northward meridional wind (20 m/s) applied everywhere causes the electron density in the downwind "leg" of a field-aligned ESF bubble to increase because of downward plasma flows. If a converging zonal wind pattern is added, it can disrupt the upward motion of an ESF bubble. The cessation of ESF-related plasma uplift ($E \times B$ upward across field lines) allows the downwind leg of the bubble to "fill in," enhancing its density above the background density, thereby leading to an airglow enhancement. Another important result from the model is that it predicts (in the northern hemisphere), at latitudes close to Arecibo, an increase in electron density between 300 and 700 km. This height range includes the region sampled by ROCSAT that shows an increase in ion density. The two other cases, 12 December 2002 and 18 December 2004, do not show the brightening occurring from the sides. It is not clear if similar mechanisms are responsible for these reversals.

[20] Recently, *Park et al.* [2008] showed the seasonal dependence of low-latitude plasma blob occurrence and found that in the northern hemisphere in the American sector the maximum occurs during December solstice, the same period that the reversals from depletions to bright structures are observed at Arecibo. The connection between the enhanced ion density and the bright airglow can be shown in Figure 6 where the satellite measures an increase in the ion density while moving above the bright airglow feature. While similar occurrence rates point to a possible connection between the plasma blob observed by ROCSAT-1 and the bright structure observed by the all-sky imager, more work is needed in order to fully understand if and how are they related.

[21] An interesting observation, not reproduced in the SAMI3/ESF simulations, and beyond the scope of this paper, is the development of secondary structures in the eastern wall of the bright regions. This is clearly noticed in the 12 December 2002 and 26 December 2003 cases in Figure 1. Secondary instabilities have been observed usually in the western wall of depleted structures. In the *Makela et al.* [2006] study, however, secondary instabilities develop in the eastern wall of the ESF-related structures at Hawaii. They were explained in terms of an E × B instability with a westward and equatorward wind acting on a density gradient pointing eastward. The same mechanism cannot be applied to the cases shown here because the structures are moving westward and the density gradient is in the same direction, i.e., a bright structure embedded in a dark background.

[22] Finally, simultaneous conjugate observations at both hemispheres using all-sky imagers will help to understand how these processes evolve. According to the results from the SAMI3/ESF simulations, a dark structure measured with a conjugate all-sky imager would become darker, rather than brighter. This could be an excellent opportunity to validate the driving mechanism proposed in the model. In order to study this phenomenon and other relevant processes occurring in the low-latitude ionosphere that will benefit from conjugate studies, Boston University installed an all-sky imager system close to the conjugate point of Arecibo at the Mercedes Observatory (34.57°S, 59.4°W, −24° mag) in Argentina.

4. Summary

[23] We have shown 630.0 nm images from the Boston University all-sky imager at Arecibo, Puerto Rico, from three different nights during December solstice periods when ESF-related airglow depletions become regions with enhanced airglow. The case we analyzed in detail, 26 December 2003, shows that the increase in brightness occurred during the reversal of the background meridional and zonal plasma drift motions, as measured by the Arecibo Incoherent Scatter Radar. ROCSAT-1 data (at a height ~570 km) show an enhancement in ion density above the bright airglow structure observed by the imager; this enhancement is accompanied by strong drifts parallel to the magnetic field, i.e., poleward and downward into the airglow layer, while outside the enhanced region the plasma moves antiparallel to B. This indicates that the enhanced airglow observed in the originally depleted structure is a consequence of plasma moving to lower altitudes and, as a result, increased emission in 630.0 nm occurs. The study by *Krall et al.* [2009] indicates that the explanation of this phenomenon could be linked to the behavior of the zonal and meridional winds. Also, the common characteristics shared by low-latitude plasma blobs and airglow enhancements, e.g., December solstice occurrence and the direction of plasma velocities, indicate a possible connection between both phenomena.

[24] **Acknowledgments.** This work was supported by NSF and ONR grants to Boston University. The Arecibo Observatory is part of the National Astronomy and Ionosphere Center, which is operated by Cornell University under a cooperative agreement with the National Science Foundation. We thank the personnel of Arecibo Observatory, in particular Raul Garcia and Jonathan Friedman, for their continuous assistance in the operation of the imaging system.

[25] Amitava Bhattacharjee thanks the reviewers for their assistance in evaluating this paper.

References

Baumgardner, J., B. Flynn, and M. Mendillo (1993), Monochromatic imaging instrumentation for applications in aeronomy of the Earth and planets, *Opt. Eng.*, *32*, 3028–3032.

Behnke, R. A. (1979), *F* layer height bands in the nocturnal ionosphere over Arecibo, *J. Geophys. Res.*, *84*, 974–978.

Cosgrove, R. B. (2007), Generation of mesoscale *F* layer structure and electric fields by the combined Perkins and Es layer instabilities, in simulations, *Ann. Geophys.*, *25*, 1579–1601.

Cosgrove, R. B., and R. T. Tsunoda (2004), Instability of the *E–F* coupled nighttime midlatitude ionosphere, *J. Geophys. Res.*, *109*, A04305, doi:10.1029/2003JA010243.

Emmert, J. T., M. L. Faivre, G. Hernandez, M. J. Jarvis, J. W. Meriwether, R. J. Niciejewski, D. P. Sipler, and C. A. Tepley (2006), Climatologies of nighttime upper thermospheric winds measured by ground-based Fabry-Perot interferometers during geomagnetically quiet conditions: 1. Local time, latitudinal, seasonal, and solar cycle dependence, *J. Geophys. Res.*, *111*, A12302, doi:10.1029/2006JA011948.

Garcia, F., M. Kelley, J. Makela, and C.-S. Huang (2000), Airglow observations of mesoscale low-velocity traveling ionospheric disturbances at midlatitudes, *J. Geophys. Res.*, *105*, 18,407–18,415.

Huba, J. D., G. Joyce, and J. Krall (2008), Three-dimensional equatorial spread F modeling, *Geophys. Res. Lett.*, *35*, L10102, doi:10.1029/2008GL033509.

Hunsucker, R. D. (1982), Atmospheric gravity waves generated in the high-latitude ionosphere: A review, *Rev. Geophys.*, *20*, 293–315.

Kelley, M. C. (1989), *The Earth's Ionosphere: Plasma Physics and Electrodynamics*, *Int. Geophys. Ser.*, vol. 43, Academic, San Diego, Calif.

Kelley, M., J. J. Makela, and A. Saito (2002), The mid-latitude *F* region at the mesoscale: Some progress at last, *J. Atmos. Sol. Terr. Phys.*, *64*, 1525–1529.

Krall, J., J. Huba, and C. R. Martinis (2009), Three-dimensional modeling of equatorial spread-F airglow enhancements, *Geophys. Res. Lett.*, *36*, L10103, doi:10.1029/2009GL038441.

Le, G., C. S. Huang, R. F. Pfaff, H. C. Yeh, R. A. Heelis, F. J. Rich, and M. Hairston (2003), Plasma density enhancements associated with equatorial spread F: ROCSAT-1 and DMSP observations, *J. Geophys. Res.*, *108*(A8), 1318, doi:10.1029/2002JA009592.

Makela, J. (2006), A review of imaging low-latitude ionospheric irregularity processes, *J. Atmos. Sol. Terr. Phys.*, *68*(13), 1441–1458.

Makela, J. J., M. C. Kelley, and M. J. Nicolls (2006), Optical observations of the development of secondary instabilities on the eastern wall of an equatorial plasma bubble, *J. Geophys. Res.*, *111*, A09311, doi:10.1029/2006JA011646.

Martinis, C., and M. Mendillo (2007), Equatorial spread F-related airglow depletions at Arecibo and conjugate observations, *J. Geophys. Res.*, *112*, A10310, doi:10.1029/2007JA012403.

Mendillo, M., H. Spence, and S. T. Zalesak (1985), Simulations studies of ionospheric airglow signatures of plasma depletions at the equator, *J. Atmos. Terr. Phys.*, *47*, 885–893.

Mendillo, M., J. Baumgardner, D. Nottingham, J. Aarons, B. Reinisch, J. Scali, and M. Kelley (1997), Investigations of thermospheric-ionospheric dynamics with 6300-Å images from the Arecibo Observatory, *J. Geophys. Res.*, *102*, 7331–7343.

Miller, C. A., W. E. Swartz, M. C. Kelley, M. Mendillo, D. Nottingham, J. Scali, and B. Reinisch (1997), Electrodynamics of midlatitudes spread F: 1. Observations of Unstable, gravity wave induced ionospheric electric fields at tropical latitudes, *J. Geophys. Res.*, *102*, 11,521–11,532.

Park, J., K. W. Min, J. J. Lee, H. Kil, V. P. Kim, H. J. Kim, E. Lee, and D. Y. Lee (2003), Plasma blob events observed by KOMPSAT-1 and DMSP F15 in the low latitude nighttime upper ionosphere, *Geophys. Res. Lett.*, *30*(21), 2114, doi:10.1029/2003GL018249.

Park, J., K. W. Min, V. P. Kim, H. Kil, H. J. Kim, J. J. Lee, E. Lee, S. J. Kim, D. Y. Lee, and M. Hairston (2008), Statistical description of low-latitude plasma blobs as observed by DMSP F15 and KOMPSAT-1, *Adv. Space Res.*, *41*, 650–654.

Perkins, F. (1973), Spread F and ionospheric currents, *J. Geophys. Res.*, *78*, 218–226.

Pimenta, A. A., Y. Sahai, J. A. Bittencourt, M. A. Abdu, H. Takahashi, and M. J. Taylor (2004), Plasma blobs observed by ground-based optical and radio techniques in the Brazilian tropical sector, *Geophys. Res. Lett.*, *31*, L12810, doi:10.1029/2004GL020233.

Pimenta, A. A., Y. Sahai, J. A. Bittencourt, and F. J. Rich (2007), Ionospheric plasma blobs observed by OI 630 nm all-sky imaging in the Brazilian tropical sector during the major geomagnetic storm of April 6–7, 2000, *Geophys. Res. Lett.*, *34*, L02820, doi:10.1029/2006GL028529.

Seker, I., J. D. Mathews, J. Wiig, P. Gutierrez, J. S. Friedman, and C. A. Tepley (2007), First results from the Penn State Allsky Imager at the Arecibo Observatory, *Earth Planets Space*, *59*(3), 165–176.

Shiokawa, K., C. Ihara, Y. Otsuka, and T. Ogawa (2003), Statistical study of nighttime medium-scale traveling ionospheric disturbances using midlatitude airglow images, *J. Geophys. Res.*, *108*(A1), 1052, doi:10.1029/2002JA009491.

Su, S.-Y., H. C. Yeh, and R. A. Heelis (2001), ROCSAT-1 ionospheric plasma and electrodynamics instrument observations of equatorial spread F: An early transition scale result, *J. Geophys. Res.*, *106*, 29,153–29,159.

Sulzer, M., N. Aponte, and S. Gonzalez (2005), Application of linear regularization methods to Arecibo vector velocities, *J. Geophys. Res.*, *110*, A10305, doi:10.1029/2005JA011042.

Tsunoda, R. (1983), On the generation and growth of equatorial backscatter plumes: 2. Structuring of the west walls of upwellings, *J. Geophys. Res.*, *88*(A6), 4869–4874.

Yokoyama, T, S. Su, and S. Fukao (2007), Plasma blobs and irregularities concurrently observed by ROCSAT-1 and Equatorial Atmosphere Radar, *J. Geophys. Res.*, *112*, A05311, doi:10.1029/2006JA012044.

N. Aponte, National Astronomy and Ionosphere Center, Arecibo Observatory, HC03 Box 53995, Arecibo, PR 00612, USA.

J. Baumgardner, C. Martinis, and M. Mendillo, Center for Space Physics, Boston University, 725 Commonwealth Avenue, Boston, MA 02215, USA. (martinis@bu.edu)

S.-Y. Su, Institute of Space Science and Center for Space and Remote Sensing Research, National Central University, No. 300, Jhongda Road, Jhongli City, Taoyuan 32001, Taiwan.